

Synthesis and characterization of undoped and Mn doped Zinc oxide

Dr jyostna chauhan¹ † Adil Aziz Khan

¹. HOD physics Rajiv Ganhi Technical University, Bhopal (M.P.)

EMAIL:jyotsnachauhan2006@gmail.com

Abstract

Mn-doped ZnO particles were synthesized using the chemical co-precipitation method. The samples were characterized using XRD, FTIR, UV-Vis, and PL spectroscopy. The average crystallite sizes, calculated using the Debye-Scherrer formula, confirmed that the particles are in the nanoscale range. XRD analysis further revealed the absence of any secondary phases or impurity peaks, indicating phase purity. Additionally, optical studies showed a decrease in the band gap with increasing Mn doping, with values ranging from 2.97 eV for Mn-doped ZnO to 2.65 eV for undoped ZnO.

Key Words:, UV-Vis absorption spectroscopy, nanocomposites, CBD

EXPERIMENTAL WORK

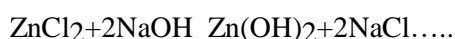
Studies have identified five common methods for synthesizing undoped and Mn-doped ZnO nanoparticles: sol-gel, solvothermal (with microwave heating), solid-state reaction, hydrothermal, and chemical precipitation. In this work, the chemical precipitation method was employed.

In a typical precipitation reaction, when silver nitrate is added to a sodium chloride solution, a white precipitate of silver chloride forms. Similarly, mixing potassium iodide with lead nitrate results in the formation of a yellow precipitate of lead iodide. Precipitation occurs when the concentration of a compound exceeds its solubility limit, which can happen due to changes in solvent composition or temperature. Rapid precipitation can also take place from supersaturated solutions.

In solid materials, precipitation can occur when the concentration of one component exceeds its solubility in the host material—often triggered by rapid quenching or ion implantation—provided the temperature is high enough to allow diffusion and phase segregation. This principle is widely used to synthesize nanoclusters in solid-state systems.

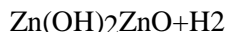
A crucial step in the precipitation process is nucleation, which involves the formation of solid particles. This requires energy to create an interface between the new solid phase and the surrounding solution, depending on their surface energies. If sufficient energy or a suitable nucleation surface is lacking, the system remains in a supersaturated state without precipitate formation.

In this study, ZnO nanoparticles were synthesized by chemical precipitation using zinc chloride and sodium hydroxide as precursor materials. The concentration ratio between these two precursors was determined based on the stoichiometric balance derived from the chemical reaction equation provided below.



Hence, 0.4M aqueous methanol solution of zinc chloride was kept under constant stirring using magnetic stirrer to completely dissolve the zinc chloride and 0.8M aqueous methanol solution of sodium hydroxide was also prepared in the same way and kept under stirring. The speed of stirring the Zinc chloride was increased after its complete dissolution and 0.8M aqueous solution of sodium hydroxide was added for 20mins in drops. The colorless solution obtained after complete addition of addition of NaOH was allowed to be under constant stirring for 2hrs and later sealed and kept overnight. After the whole process Zinc hydroxide with some unknown impurities assumed settled at the bottom and the excess mother liquor obtained on top was removed. The remaining solution was centrifuged for 5mins and the precipitate obtained was washed five times with

deionized water and methanol to remove the by products which were bound with the Zinc hydroxide and then dried in air atmosphere. After drying Zn(OH)_2 is completely converted to ZnO explained by the equation below:



Synthesis of Mn-doped ZnO Nanoparticles

To synthesize ZnO nanoparticles, two key precursors are required—one providing zinc and the other oxygen. For the preparation of Mn-doped ZnO, zinc sulfate, manganese sulfate, and sodium hydroxide were used as the starting materials. During nanoparticle formation, it is essential to add a capping agent to prevent uncontrolled particle growth. Without it, the particles continue to grow beyond the nanometer scale. In this synthesis, **ethylene glycol (EG)** was used as the capping agent to maintain nanoscale dimensions.

Analytical-grade reagents were utilized. A 0.2 M solution of zinc sulfate heptahydrate ($\text{ZnSO}_4 \cdot 7\text{H}_2\text{O}$) and a 0.2 M solution of manganese sulfate monohydrate ($\text{MnSO}_4 \cdot \text{H}_2\text{O}$) were each prepared separately in 30 ml of distilled water and stirred for 30 minutes at room temperature. These solutions were then combined under continuous stirring. A 1 M aqueous solution of NaOH was added dropwise until the pH reached 10, initiating precipitation.

Immediately after NaOH addition, 10 ml of ethylene glycol was introduced to cap the nanoparticles. The mixture was stirred for 20 hours at room temperature to ensure uniformity. The precipitate was collected by centrifugation. The resulting material was washed repeatedly with deionized water until the pH of the solution was neutral (around 7). The washed sample was dried at 150°C and then ground into a fine powder. Finally, it was calcined at 400°C for 3 hours in a muffle furnace to obtain the Mn-doped ZnO nanoparticles.

Data collection and structure solution :

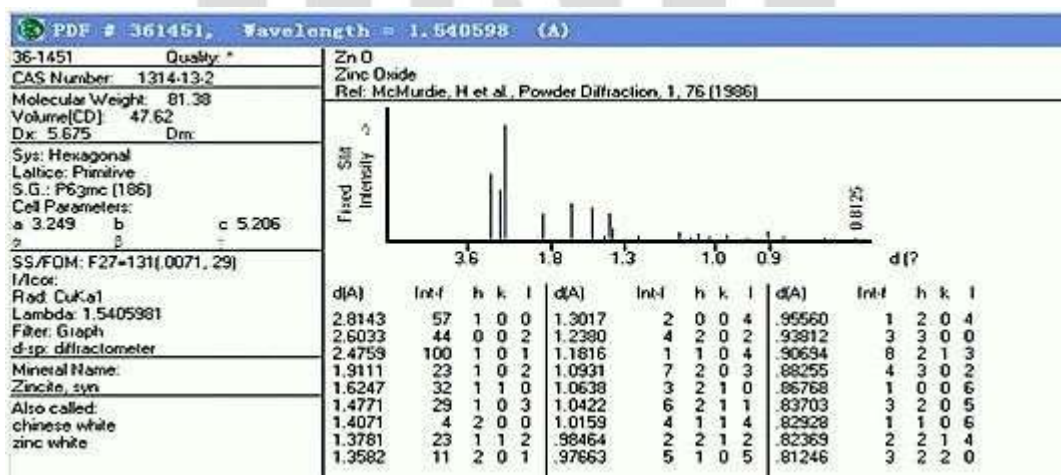


Fig – 1 XRD reference data for ZnO wurtzite JCPDS No. 36-1451

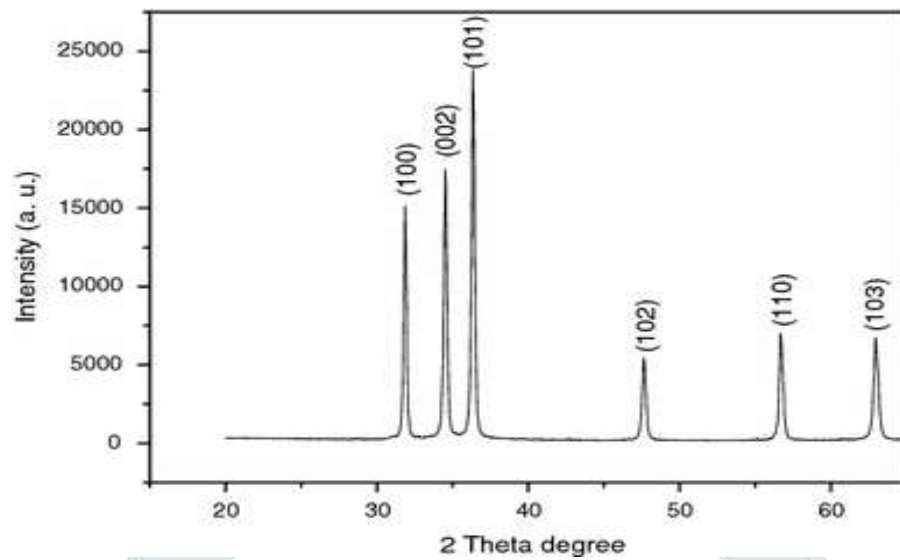


Fig – 2 XRD Spectra of Undoped ZnO nanoparticles

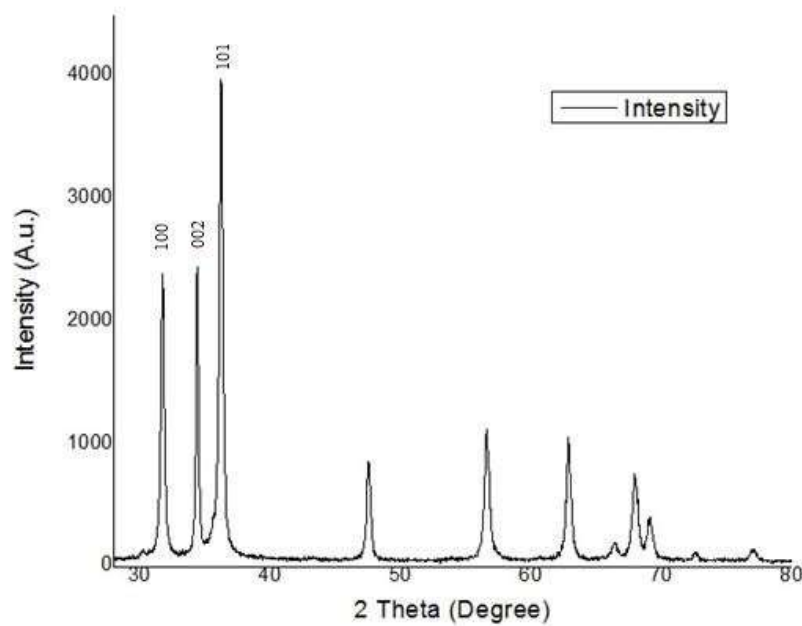


Fig – 3 XRD Spectra of Mn doped ZnO nanoparticles

Result and discussion: , we have taken Undoped ZnO and Mn doped ZnO and calculated their different parameters.

a. Crystallite Size: The X-ray diffraction of the samples were recorded by an X-ray diffractometer with a $\text{CuK}\alpha$ radiation ($\lambda = 1.54060 \text{ \AA}$) in a range of 2θ from 30° to 80° . The top three peaks are only produced at 2θ ranging from 30° to 38° which further corresponds to the crystal planes (100), (002) and (101) for Mn doped ZnO and for Undoped ZnO, $\text{CuK}\alpha$ radiation ($\lambda = 1.54060 \text{ \AA}$) in a range of 2θ from 20° to 70° . The top three peaks are only produced at 2θ ranging from 30° to 38° which further corresponds to the crystal planes (100), (002) and (101) as of Mn doped. The broadening of the diffraction peak in the xrd pattern indicates the formation of the nanocrystallinity. Using Debye-Scherrer formula, the crystalline size of the sample was calculated from full width at half maxima of XRD pattern shown in Fig 2 and Fig 3. The average nanocrystallite size is calculated by the formula,

$$D = 0.9 \lambda / \beta \cos \theta \dots \text{Eq (2)}$$

Where λ is the wavelength of the incident ray, θ is the Bragg's angle and β is the full width at half maxima.

b Non Uniform Strain:

We have also studied the change in non-uniform strain (η) with particle size using the Hall equation,

$$\beta \frac{\cos \theta}{\lambda} = \frac{1}{t} + 2\eta \frac{\sin \theta}{\lambda} \dots \text{Eq (3)}$$

where, ' λ ' is the wavelength of x-ray used for scattering experiment and ' t ' is the particle size and β is the line broadening.

c. Dislocation Density: The dislocation density (δ) which represents the amount of defects in the sample is calculated using the relation

$$\delta = 1/D^2 \dots \text{Eq (4)}$$

where D is the average crystallite size where λ is the X-ray wavelength (here $\lambda = 1.54060 \text{ \AA}$) and θ is the Bragg's angle.

d. Average Strain: The average strain of the nanoparticles is calculated using following equation

$$\epsilon = \beta / 4 \tan \theta \dots \text{Eq (5)}$$

where ϵ = Average strain, β = FWHM, θ = Bragg's Angle

Calculation Table 1 for Undoped Zno		
Sr.No	Properties	Value
1.	Crystallite Size (nm)	21
2.	FWHM(degree)	36.236
3.	Non Uniform Strain	0.0745
4.	Dislocation Density δ (lines/m ²)	2.26×10^{15}
5.	Average Strain	17.498

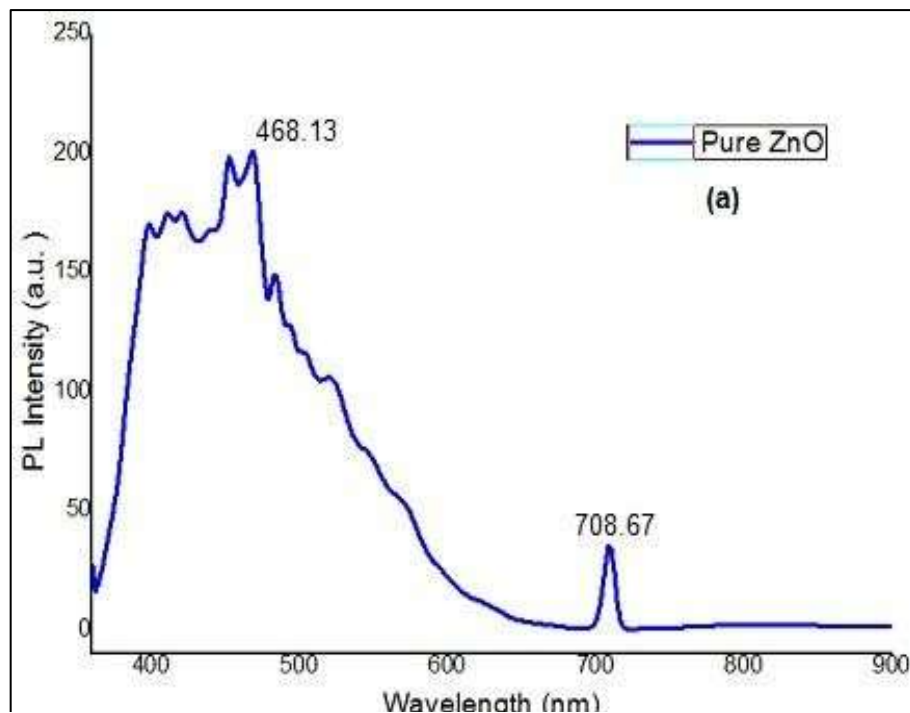
Calculation Table 2 for Mn doped Zno		
Sr.No	Properties	Value
1.	Crystallite Size (nm)	27
2.	FWHM(degree)	36.736
3.	Non Uniform Strain	0.03
4.	Dislocation Density δ (lines/m ²)	1.365×10^{15}
5.	Average Strain	13.776

PL Spectroscopy

The photoluminescence intensity depends strongly on Mn concentrations. Intensity is maximum for low concentrations of Mn and further it can be decreased together with the broadening of the FWHM (Full Width at Half Maximum) as a function of Mn content. The higher concentration of

Mn induces a high density of defects, which acts as non-radiative recombination centres and reduces the intensity of emitted light.

Figure 4 PL for pure ZnO phase



The energy gap is calculated is using the equation for photon energy in terms of eV and μm .

$$\lambda = 1.24/E_g \mu\text{m} \dots \text{Eq (12)}$$

and is found to be **2.65 eV for Undoped ZnO** and **2.97 eV for Mn doped ZnO**

FTIR Spectroscopy:

The FTIR spectrum of Undoped ZnO and Mn doped ZnO at room temperature is shown in below figure. 5 and 6. These spectrums shows the IR absorption due to the various vibration modes

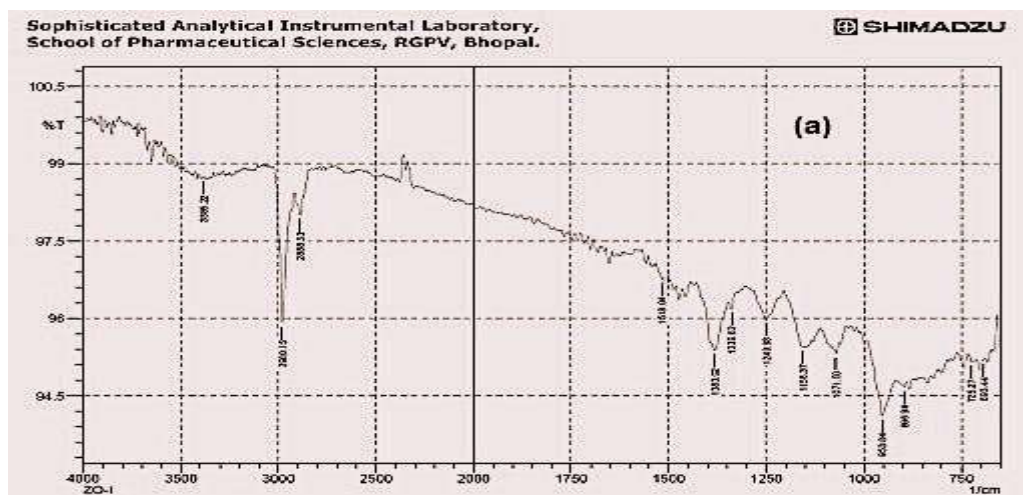


Fig – 5 FTIR of Undoped ZnO

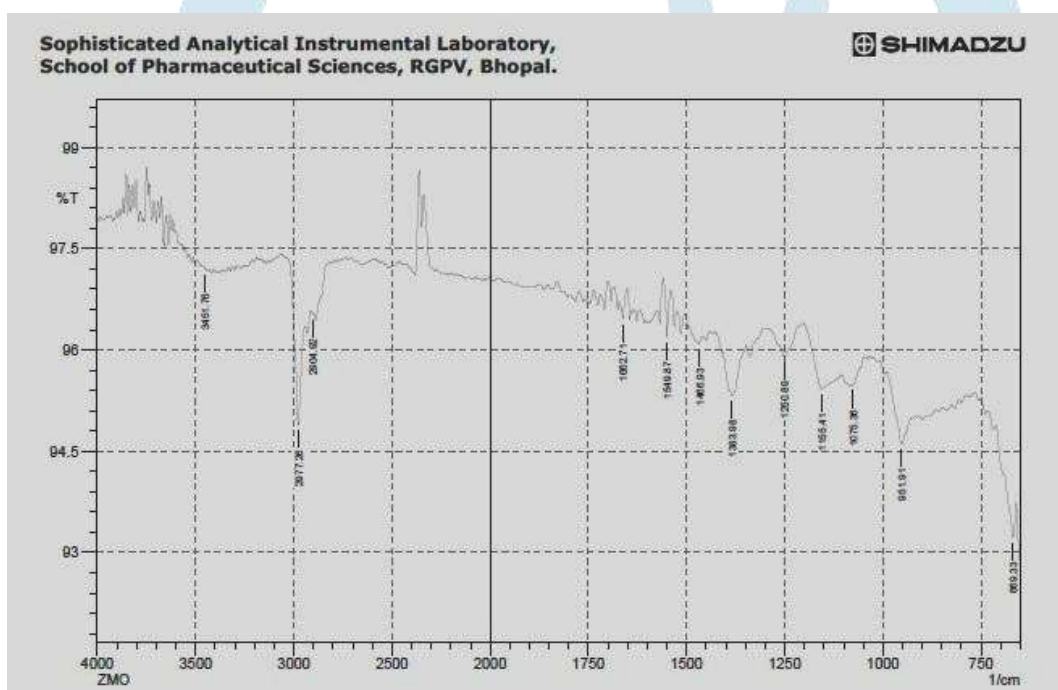


Fig – 6 FTIR of Mn doped ZnO

UV-Vis Spectroscopy:

UV-Vis spectra of undoped and Mn doped ZnO observed in the 200-800nm range. Before the UV Characterization we have dissolve 10mg of each sample in the 50ml DI separately to form a monodispersed solution. After this each sample was sonicated for 30 min. Both samples are not having any peak in the visible region. A UV-Vis spectrum is used for the band gap calculation but it requires the wavelength at which spectra start to take off. But it is difficult to obtain take off wavelength manually, so we have only information about the peak wavelength where absorption is highest and value of the absorption. Undoped ZnO has the peak absorbance of 1.143 at the

wavelength 372nm. Manganese doped ZnO has highest absorbance of 0.747 at the wavelength 376nm. Shown in fig 7 and 8.

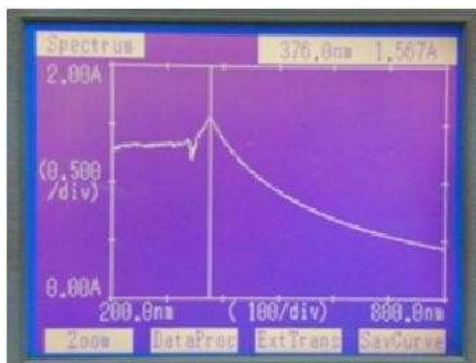


Fig – 7 UV spectroscopy of Undoped ZnO

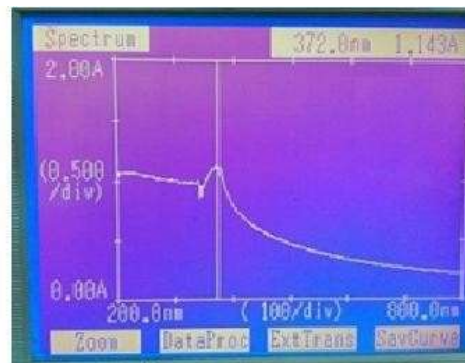


Fig –8 UV spectroscopy of Mn doped ZnO

CONCLUSION: In summary, pure and Mn-doped ZnO nanoparticles were successfully synthesized using the chemical precipitation method. The Mn-doped ZnO system is particularly promising due to the wide bandgap of the ZnO host material and the high solubility of Mn ions within the ZnO matrix. Additionally, Mn-doped ZnO has garnered significant interest owing to ongoing debates regarding the presence and origin of room-temperature ferromagnetism in such systems. The crystallite sizes of the undoped and Mn-doped ZnO were determined to be approximately 21 nm and 27 nm, respectively. The optical band gaps were calculated to be 2.65 eV for undoped ZnO and 2.97 eV for Mn-doped ZnO.

References –

- [1] K. Zamani, *Proc. SPIE* 4608,266 (2002).
- [2] A. Vilan and D. Cahen, *Tmnds in Biotechnology* 20,22 (2002). R.F. Service, *Science* 293, 782 (2001).
- [4] K. Sato, H. Katayama-Yoshida, Japan. *J. Appl. Phys. Part 2* 39 (2000).
- [5] T. Dietl, H. Ohno, F. Matsukura, J. Cibert, D. Ferrand, *Science* 287 (2000).
- [6] S.J. Pearton, C.R. Abernathy, M.E. Overberg, G.T. Thaler, D.P. Norton, N. Theodoropoulou, A.F. Hebard, Y.D. Park, F. Ren, J. Kim, L.A. Boatner, *J. Appl. Phys.* 93 (2003).
- [7] R. Janisch, P. Gopal, N.A. Spaldin, J. Phys.: *Condens. Matter* 17 (2005).
- [8] Z. Jin, T. Fukumura, M. Kawasaki, K. Ando, H. Saito, T. Sekiguchi, Y.Z. Yoo, M. Murakami, Y. Matsumoto, T. Hasegawa, H. Koinuma, *Appl. Phys. Lett.* 78 (2001).
- [9] T. Fukumura, Z. Jin, M. Kawasaki, T. Shono, T. Hasegawa, S. Koshihara, H. Koinuma, *Appl. Phys. Lett.* 78 (2001).
- [10] J.M.D. Coey, M. Venkatesan, C.B. Fitzgerald, *Nature Mater.* 4,173(2005). [11] N.H. Hong, J. Sakai, V. Brize, J. *Phys.: Condens. Matter* 19, 036219 (2007).
- [12] D. Segets, J. Gradl, R.K. Taylor, V. Vassilev, W. Peukert, *ACS Nano* 3, 1703–1710.(2009)
- [13] R. Guo, X. Lou, J. Sens. *Trans. Technol.*,(1991)

- [14] R.Wahab, S.G. Ansari, Y.S. Kim, H.K. Seo, H.S. Shin, *Appl. Surf. Sci.* , 253, 7622,7626 (2007)
- [15] D. C. Look, B. Clafin, Y. I. Alivov, S. J. Park, *Phys. Stat. Sol. (a)* 201 (2004). [16] S. J. Pearton, D. P. Norton, K. Ip, Y.W. Heo, T. Steiner, *Prog. Matter. Sci.* 50 (2005).
- [17] U. Özgür, Y. I. Alivov, C. Liu, A. Teke, M. A. Reshchikov, S. Doñuan, V. Avrutin, S. J. Cho, H. Morkoç, *J. Appl. Phys.* 98 (2005).
- [18] S. Adachi, *Properties of Group-IV, III-V and II-VI Semiconductors*, John Wiley and Sons, (2005).
- [19] D. I. Florescu, L. G. Mourokh, F. H. Pollak, D. C. Look, G. Cantwell, X. Li, J. *Appl. Phys.* 91 (2002).
- [20] A. Holleman, F. Arnold, S. Wiberg and L. Egon Nils "Mangan". *Lehrbuch der Anorganischen Chemie* (1985).
- [21] K. Lide, R. David, *Magnetic susceptibility of the elements and inorganic compounds*, in *Handbook of Chemistry and Physics*, (2004).
- [22] R.B. Temple, G.W. Thickett "The formation of manganese(v) in molten sodium nitrite" (PDF). *Australian Journal of Chemistry*, (1972).
- [23] P.W. Cyr, M. Tzolov, M.A. Hines, I. Manners, E.H. Sargent, G.D. Scholes, *Quantum dots in a metallopolymer host: studies of composites of polyferrocenes and CdSe nanocrystals*, *J. Mater.Chem.*, (2003)
- [24] H. Fendler, F.C. Meldrum, *The colloid chemical approach to nanostructured materials*, *Adv. Mater.*, (1995).
- [25] N. Lopez, T.V.W. Janssens, B.S. Clausen, Y. Xu, M. Mavrikakis, T. Bligaard, J.K. Norskov, *On the origin of the catalytic activity of gold nanoparticles for low- temperature CO oxidation*, *J. Catal.* (2004)
- [26] T. Chakraborty, *Quantum Dots, Density of States*, (1999)
- [27] U. Shmueli, *International Tables for Crystallography, vol. B, Second Edition*, (2001).
- [28] A.J.C. Wilson, E Prince , *International Tables for Crystallography, vol. C, Second Edition*, (1999).
- [29] B.D. Cullity, *Elements of X-ray Diffraction*, (1978).
- [30] H.P. Klug and L.E.S Alexander, *X-ray Diffraction Procedures. For Polycrystalline and Amorphous Materials*, 2nd ed., New York, John Willey and Sons (1974).